

## Effects of Operational Parameters on the TiO<sub>2</sub> and TiO<sub>2</sub>/Ag Core-Shell Photocatalysis System for Decolorizing AR14

<sup>1,2</sup>Masood Hamadani, <sup>3</sup>Mohsen Behpour, <sup>4</sup>Asra Sadat Razavian and <sup>1</sup>Vahid Jabbari

<sup>1</sup>Institute of Nanosciences and Nanotechnology, University of Kashan, Kashan, I.R. Iran

<sup>2</sup>Department of Physical Chemistry, Faculty of Chemistry, University of Kashan, Kashan, I.R. Iran

<sup>3</sup>Department of Chemistry, Faculty of Science, University of Kashan, Kashan, I.R. Iran

<sup>4</sup>Department of Analytical Chemistry, Faculty of Science, University of Kashan, Kashan, I.R. Iran

**Abstract:** In this work, nanostructured titanium dioxide (TiO<sub>2</sub>) thin films have been prepared on glass substrates using a facile layer-by-layer dip-coating method. The nano-layer surface was characterized by X-ray diffraction (XRD) and scanning electron microscopy (SEM) analysis. It was observed that degradation of Acid Red 14 (AR14) depend on several parameters such as pH, the coating of silver and dipping times. In addition, TiO<sub>2</sub> from TiO<sub>2</sub>/Ag demonstrated photocatalysis performance when irradiated and the Ag carrier further showed an electron-scavenging ability to mitigate electron-hole pair recombination, which can improve the photocatalytic efficacy. With the oxidization and electron-scavenging ability of Ag and the photocatalysis ability of TiO<sub>2</sub>, TiO<sub>2</sub>/Ag can decolor AR14 more efficiently than TiO<sub>2</sub>.

**Key words:** Titanium dioxide • Silver • Electron-Scavenging • Photocatalysis • Decolorization

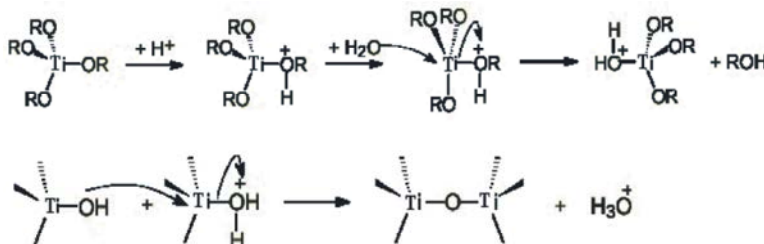
### INTRODUCTION

With increasing environment protection awareness in recent years, environment pollution issues have become major concerns; among these issues, wastewater color is very important. Besides causing color contamination as well as affecting water body clarity and transmittance, some toxic dyes also pose hazards to organisms in water bodies [1]. Common dye wastewater treatment methods include biological (activated sludge) and chemical processes (the Fenton process and coagulation) [2,3]. Coagulation processes and the Fenton process have low equipment costs, but produce large amounts of sludge; thus, additional costs for sludge treatment are required. Using activated carbon to physically adsorb wastewater color showed a significant effect, but it requires frequent replacement and the treatment expense is so high that its application is not practical [4]. The above problems can be solved by using a titanium dioxide (TiO<sub>2</sub>) plus ultraviolet (UV) photocatalysis method to remove dye color.

The anatase TiO<sub>2</sub> polymorph is the most important photocatalyst used today. Since the discovery of its photocatalytic activity by UV irradiation in 1972 [5], many studies have been developed with this material in the photodegradation of phenols [6], dyes [7],

microorganisms [8], herbicides [9] and a variety of organic contaminants. Its band gap energy of 3.2eV provides the formation of electron-hole pairs which may be activated with wavelengths shorter than 380nm. Therefore, many efforts have been made to enhance the activation of TiO<sub>2</sub> at wavelengths closer to those of visible light. These efforts include methods such as doping of TiO<sub>2</sub> with transition metals, rare earths, metals, non-metallic anions, and surface modification (impregnation and deposition) with noble metals [10,11]. Regularly, surface modification consists of nanoparticles embedded or anchored to the surface of TiO<sub>2</sub>, trapping of electrons being its main function, thereby decreasing the recombination of the electron-hole pairs. For noble metals, silver is one of the most suitable for industrial applications due to its low cost and ease of preparation. Nanoparticles of silver anchored to the surface of TiO<sub>2</sub> have proven to be highly efficient, favoring the activation of the titania under visible light irradiation [12,13].

The present study deals with an examination of photoadsorption, photoreduction and photodeposition of silver clusters on TiO<sub>2</sub> particles immobilized on the glass substrates. Experimental results have shown that the preparation of high transparent TiO<sub>2</sub> thin film by dip coating method needs to control pH, thickness of the film and Ag coating.



Scheme 1: Mechanism of poly-condensation reactions of  $\text{Ti}(\text{OBu})_4$  precursor in the acidic environment.

## Experimental

### $\text{TiO}_2$ Sol Preparing and Dip-Coating on the Glass

**Substrates:** All the chemicals were purchased from Merck and were used without any further purification. Deionized water was obtained from ultra pure water system (type smart-2-pure made in TKA Company, Germany). 3.6 ml of  $\text{Ti}(\text{OBu})_4$  was mixed well with 5 ml:2 ml ethanol:water, chilled in ice bath, then 0.03 M  $\text{HNO}_3(\text{aq})$  was added slowly into it with vigorous stirring. The mixture was stirred at ice bath for 4 h, kept in refrigerator for storage. For poly-condensation reactions of  $\text{Ti}(\text{OBu})_4$  precursor, the process can be written as Scheme 1. The Ag-coated  $\text{TiO}_2$  films were prepared by the incipient wet impregnation with 0.0004 M  $\text{AgNO}_3$  on  $\text{TiO}_2$  films.

**Thin Films Characterization:** The XRD patterns were recorded on a Philips X'pert Pro MPD model X-ray diffractometer using  $\text{Cu K}\alpha$  radiation as the X-ray source. The diffractograms were recorded in the  $2\theta$  range of  $10-80^\circ$ . The average crystallite size of anatase phase was determined according to the Scherrer equation. The morphology and size of nanoparticles was characterized using scanning electron microscope (SEM) (Philips XL-30ESM). The extent of AR14 degradation was monitored using UV-Vis spectrophotometer (Perkin Elmer Lambda 2S).

### Evaluation of Photocatalytic Activity of the Samples:

The experiments of the photocatalytic decomposition of AR14, with application of the immobilized catalyst bed were conducted in the laboratory scale apparatus. The UV source was 400W Osram lamps for experiments. The photocatalytic degradation was carried out with 100mL aqueous AR14 solution (10ppm). The degradation percentage of AR14 in the reaction process could be calculated by the following formula:

Where  $C_t$  is the concentration of AR14 after t min and  $C_0$  is the initial concentration.

## RESULTS AND DISCUSSION

**XRD Analysis:** The nanocrystalline anatase structure was confirmed by (101), (004), (200), (105) and (211) diffraction peaks [14] as shown in Figure 1. Typical peaks in XRD pattern are observed at  $2\theta$  values  $25.28^\circ$ ,  $38.08^\circ$  and  $47.92^\circ$ , which assigned to 101, 004 and 200 planes, respectively, while the main peaks of rutile and brookite phases are at  $2\theta = 27.4^\circ$  (110 plane) and  $2\theta = 30.8^\circ$  (121 plane). Therefore, brookite phase has not been detected. In order to obtain photocatalytic activity, it is necessary to make proper anatase nanostructure, but it is evident that some rutile phase could improve the photocatalytic effect [15]. The average size of nanoparticles was estimated from the Scherrer equation was around 15-25 nm.

**Characteristic of  $\text{TiO}_2$  Films by SEM:** We examined the quality of the  $\text{TiO}_2$  thin films after dip-coating the glass beads into the  $\text{TiO}_2$  suspension solution one ( $\text{TiO}_2$ -1) or five times ( $\text{TiO}_2$ -5). Figure 2(a), (b) denotes SEM micrographs of  $\text{TiO}_2$  films fabricated on glass substrate, having different layers. As shown from microstructural observations, the thickness of film and surface defects increases in accordance with number of dipcoating. Cracking was less extensive in thinner films while very thick films which were produced using viscous solutions tended to peel off the substrate completely [16].

The second coating route was then carried out on the calcinated thin films to get a homogeneous and complete coated layer. SEM micrographs of the  $\text{TiO}_2$  thin films calcinated at  $550^\circ\text{C}$  temperature, is shown in Figure 3.

The Figure 4 shows SEM images of the silver particles coated on the  $\text{TiO}_2$ -5 thin film surface. The aggregated phenomena by Ag on the  $\text{TiO}_2$  may be due to the electrostatic attraction. Comparing bare  $\text{TiO}_2$  (Figure 3) and  $\text{TiO}_2$  coated electrode after Ag deposition, it can be seen that the Ag nano-clusters were formed and distributed at the films surface in a form of porous and sphere-like network of high roughness and complexity.

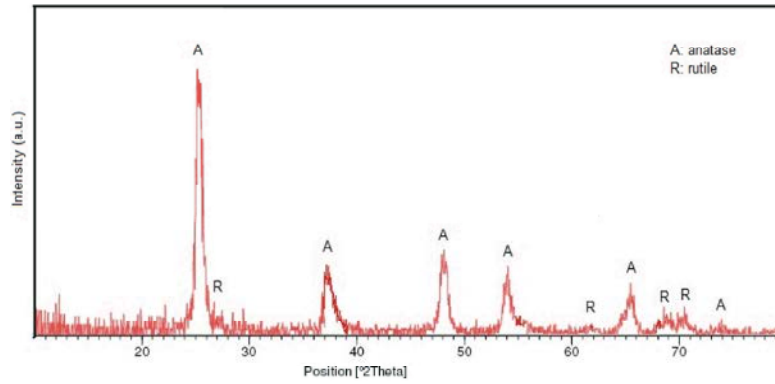


Fig. 1: The XRD Patterns of TiO<sub>2</sub>-5 thin film.

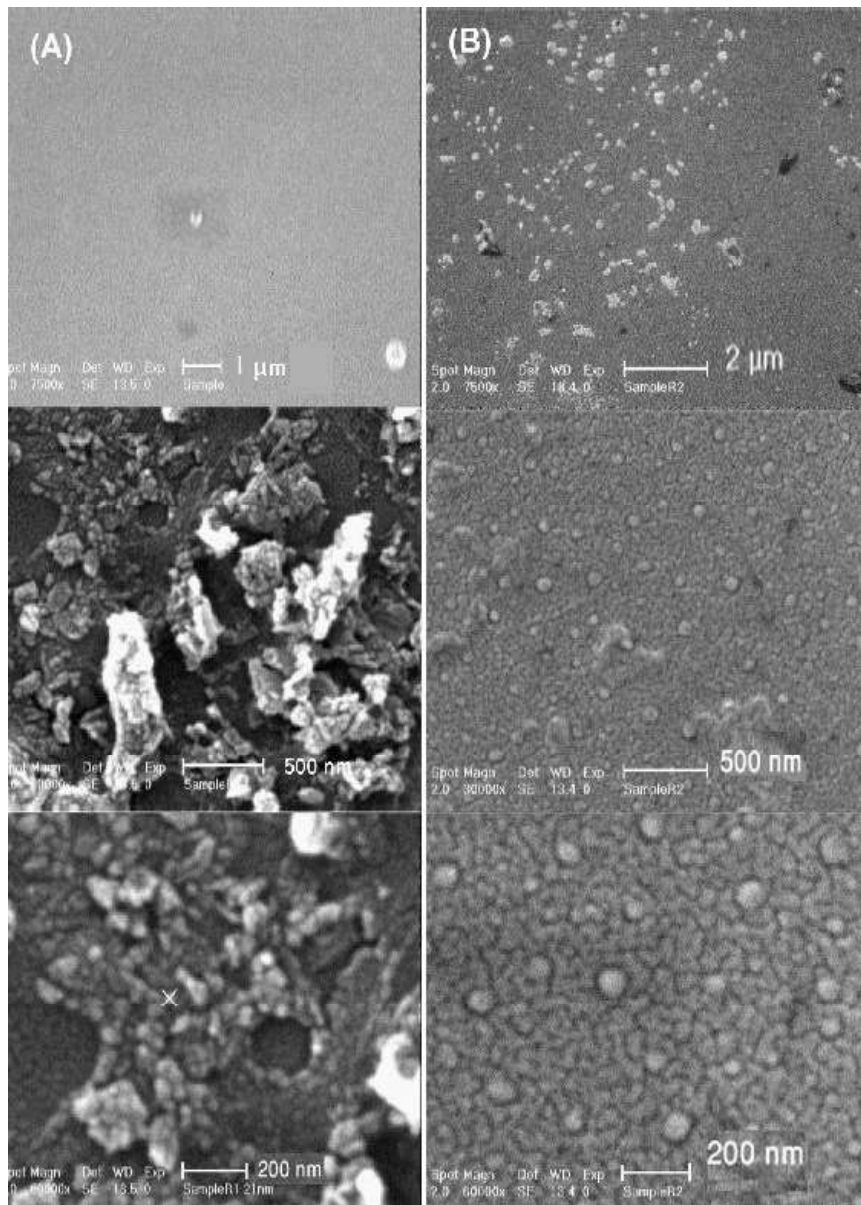


Fig. 2: The SEM images of TiO<sub>2</sub> thin films dip-coated after one (a) and five times dip-coating (b).

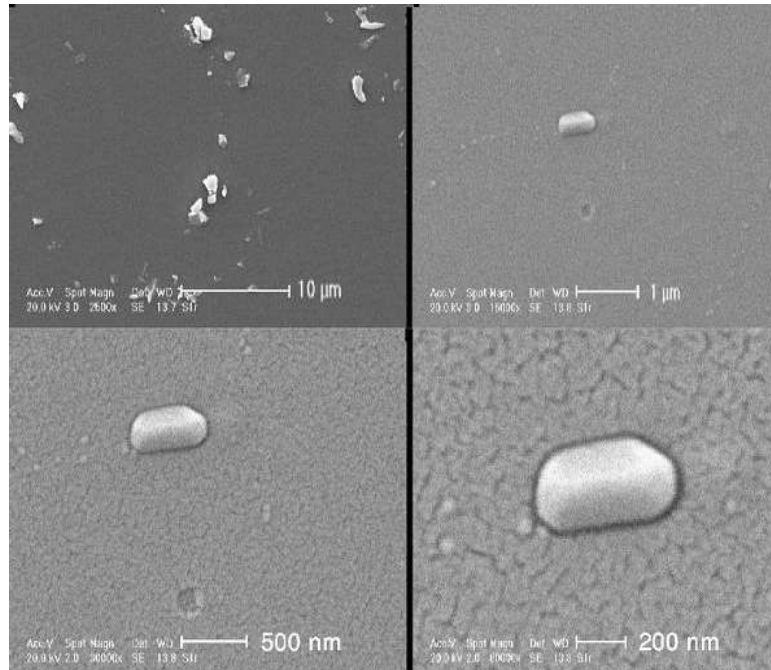


Fig. 3: The SEM images of TiO<sub>2</sub> thin films dip-coated at one (a), and five times (b) calcinated in the 550 °C.

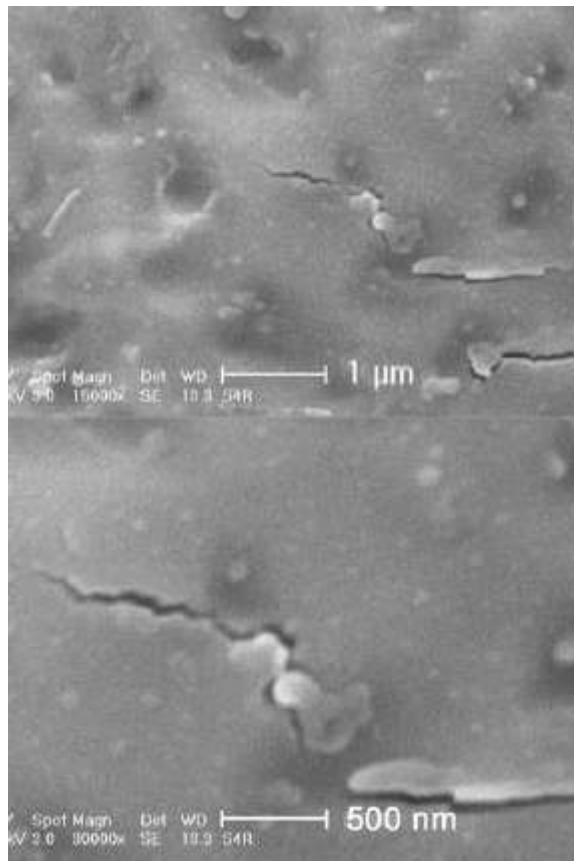
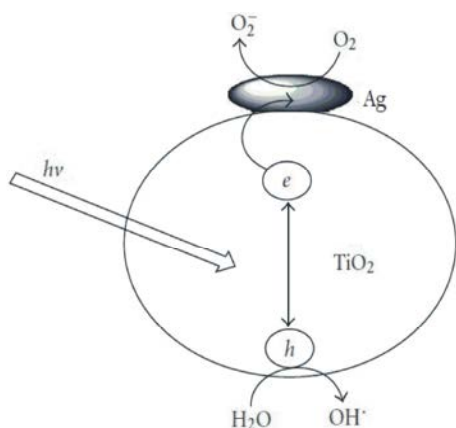


Fig. 4: The SEM images of Ag-coated TiO<sub>2</sub>-5 thin film. TiO<sub>2</sub> film were immersed in 0.004M AgNO<sub>3</sub> solution and irradiated by UV for 2.5 h.

Table 1: The photocatalytic effect on degradation of AR14 with TiO<sub>2</sub> thin films dip-coated in one (TiO<sub>2</sub>-1), five times (TiO<sub>2</sub>-5), and degradation of AR14 by Ag-coated TiO<sub>2</sub> (Ag-TiO<sub>2</sub>-5).

Sample Type	UV irradiation time (h)				
	1	2	3	4	5
TiO <sub>2</sub> -1	11	22	31	39	45
TiO <sub>2</sub> -5	20	42	56	63	68
Ag-TiO <sub>2</sub> -5	18	52	81	94	98



Scheme 2: Interfacial charge transfer process of silver-doped TiO<sub>2</sub> nanocomposites under the irradiation of UV light.

**Photocatalytic Activity of TiO<sub>2</sub> and Ag-Coated TiO<sub>2</sub> Films:** Table 1 presents the results obtained during photocatalytic decomposition of AR14 under UV light. The best decomposition results were obtained for Ag/TiO<sub>2</sub> removal was equal to 74%. In this case, TiO<sub>2</sub>-5 was more active than TiO<sub>2</sub>-1 catalyst. The differences in photocatalytic activity could be contributed from the differences in phases present, particle and surface morphology, and surface area [17].

As shown in Table 1, after modification by Ag, the catalytic activity of the TiO<sub>2</sub> layers were improved compared with the bare TiO<sub>2</sub> layer, because Ag coated TiO<sub>2</sub> itself has both photocatalysis and oxidization activities provided by TiO<sub>2</sub> and Ag, respectively, to decolorize dye. Furthermore, Ag in Ag-coated TiO<sub>2</sub> acted as an electron scavenger, and delayed electron-hole pair recombination derived from excitation of irradiated TiO<sub>2</sub>, thus promoting photocatalytic decolorization. That means Ag<sup>+</sup> acts as a good electron trapper, therefore Ag-TiO<sub>2</sub> has a slowest electron-hole recombination rate and highest catalytic activity as shown in Scheme 2 [18].

## CONCLUSION

The immobilization of Ag on the TiO<sub>2</sub> and deposition on glass sheets was achieved successfully by dip-coating processing. TiO<sub>2</sub> showed photocatalysis properties in the presence of UV irradiation and Ag from the TiO<sub>2</sub>/Ag also played a role as an electron scavenger, delaying the combination of electron-hole pairs. In the photocatalytic process, part of the electrons excited from the irradiated TiO<sub>2</sub> transformed the oxidation state of Ag to metallic Ag, which revived the oxidation activity. Thus these described characteristics enhanced the photocatalytic activity of TiO<sub>2</sub>/Ag on AR14 decolorization to a higher level than with commercial TiO<sub>2</sub>. In addition, the heavier Ag carrier improved the solid-liquid separation of nano-TiO<sub>2</sub>, thus contributing to TiO<sub>2</sub>/Ag being more suitable for application in slurry systems for photocatalytic water treatment. In addition, preparation of the photocatalyst is very simple, and the cost is economical, too.

## ACKNOWLEDGMENT

The authors gratefully acknowledged the financial support of Iran government grant for the financial support of this work which made the study possible.

## REFERENCES

1. Kabil, A.S., 2000. Chlorotriazine reactive azo red 120 textile dye induces micronuclei in fish. *Ecotox. Environ. Saf.*, 47: 149-155.
2. Lin, S.H. and M.L. Chen, 1997. Treatment of textile wastewater by chemical methods for reuse, *Water Res.*, 31: 868-876.
3. Ahmad, A.L. and S.W. Puasa, 2007. Reactive dyes decolorization from an aqueous solution by combined coagulation/micellar-enhanced ultrafiltration process, *Chem. Eng. J.*, 132: 257-265.
4. Ahmaruzzaman, M., 2008. Adsorption of phenolic compounds on low-cost adsorbents: a review, *Adv. Colloid Interface Sci.*, 143: 48-67.

5. Honda, K. and A. Fujishima, 1972. *Nature*, 238: 37-38.
6. Ding, Z., G.Q. Lu and P.F. Greenfield, 2000. *J. Phys. Chem., B*, 104: 4815.
7. Pekakis, P.A., N.P. Xekoukoulotakis and D. Mantzavinos, 2006. *Water Res.*, 40: 1276.
8. Josset, S., J. Taranto, N. Keller, V. Keller, M.C. Lett, M.J. Ledoux, V. Bonnet and S. Rougeau, 2007. *Catal. Today*, 129: 215.
9. Konstantinou, I.K., V.A. Sakkas and T.A. Albanis, 2001. *Appl. Catal., B*, 34: 227.
10. Paola, A.D., G. Marci, L. Palmisano, M. Schiavello, K. Uosaki, S. Ikeda and B. Ohtani, 2002. *J. Phys. Chem., B*, 106: 637.
11. Colón, G., J.M. Sánchez-España, M.C. Hidalgo and J.A. Navío, 2006. *J. Photochem. Photobiol., A*, 179: 20.
12. VanGrieken, R., J. Marugán, C. Sordo, P. Martínez and C. Pablos, 2009. *Appl. Catal., B*, 93: 112.
13. Yang, X., F. Ma, K. Li, Y. Guo, J. Hu, W. Li, M. Huo and Y. Guo, 2010. *J. Hazard. Mater.*, 175: 429.
14. Qamar, M., M. Saquib and M. Muneer, 2005. *Dyes Pigm.*, 65: 1-9.
15. Takahashi, Y. and Y. Matsuoka, 1988. *J. Mater. Sci.*, 23: 2259.
16. Subramanian, V., E.E. Wolf and P.V. Kamat, 2003. *Langmuir*, 19: 469-474.
17. Kim, D.J., S.H. Hahn, S.H. Oh and E.J. Kim, 2002. *Materials Letters*, 57: 355- 360.
18. Barati, N., M.A. Faghihi Sani, H. Ghasemi, Z. Sadeghian and S.M.M. Mirhoseini, 2009. *Applied Surface Sci.*, 255: 8328-8333.